Anomalous Hall Effect in *Gd*-doped $La_{2/3}Ca_{1/3}MnO_3$

M. Jaime, H. Hardner, M.B. Salamon, M. Rubinstein[†], P. Dorsey[†] and D. Emin[‡]

Department of Physics and Materials Research Laboratory

University of Illinois at Urbana-Champaign, Urbana, IL 61801

[†]*U.S. Naval Research Laboratory, Washington D.C. 20307-5000*

[‡]*Sandia National Laboratories, Albuquerque, New Mexico 87185*

(October 16, 1996)

Abstract

Ceramic samples of composition $(La_{1-x}Gd_x)_{2/3}Ca_{1/3}MnO_3$ were prepared and used as targets to grow films onto $LaAlO_3$ substrates by pulsed laser deposition. The electrical resistance and thermopower, measured *vs* temperature and applied magnetic fields indicate transport dominated by positive small polarons in the high temperature paramagnetic state. The Hall effect was measured in 0.5 μm thick films of composition $x = 0$ and $x = 0.25$. No evidence for extraordinary Hall effect was found in the paramagnetic regime. Instead, the magnitude of the Hall coefficient decreases exponentially with temperature. This behavior and its anomalous negative sign are interpreted to result from face-diagonal hopping of small polarons in the Mn sublattice.

PACS: 75.50Pp; 72.20.My; 71.38.+i

This work was supported by the United States Department of Energy under Contract DE-AC04-94AL 85000. Sandia is a multiprogram laboratory operated by Sandia Corporation, a Lockheed Martin Company, for the United States Department of Energy.

The study of the negative magnetoresistance in thin films samples of oxide perovskites $A^{3+}_{1-c}B^{2+}_{c}MnO_3$, presently known as manganites, produced an authentic renaissance of the field. [1] Materials where A^{3+} is an rare earth (La, Y, Pr, Nd) and B^{2+} an alkaline earth or metal (Ca, Ba, Sr, Pb) exhibit so called colossal magneto-resistance (CMR) due to the broadening of the transition from a ferromagnetic conductor to a paramagnetic semiconductor in applied magnetic fields. The replacement of A^{3+} with B^{2+} causes the Mn^{3+} to give up its e_g electron transforming into Mn^{4+} and consequently increasing the Mn-O bond length (also known as Jahn-Teller effect), locally distorting the lattice and creating a hole-like electronic state. Similar results in doped EuO [2] were attributed to the shrinking of extended electronic states into small polarons when the temperature is raised through the ferromagnetic transition temperature (T_c).

Experimental evidence for small-polaron conduction was found [3] in laser ablated films (A = La, B = Ca and $c = 1/3$), the signature being that the thermopower $S \propto E_s/k_BT$, with E_s much smaller than the comparatively large activation energy E_σ of the electrical conductivity. Indeed, Holstein predicted that the thermally activated drift mobility of small polarons causes E_σ to differ from E_s in an amount equal to one half of the formation energy of polarons. [4] It is now widely believed [5] that the metal B^{2+} content controls the density of charge carriers in manganites, producing large changes in the conductivity and the metal-insulator transition at T_c. On the other hand, rare earth substitutions A^{3+} affect T_c through further tilting of oxygen octahedra, [6] decreasing the Mn-O-Mn bond angle, and changing the phonon spectrum at constant doping, making such samples suitable for the study of charge self-localization. With this purpose in mind polycrystalline samples of nominal composition $(La_{1-x}Gd_x)_{2/3}Ca_{1/3}MnO_3$ with $x = 0$, 0.25 and 0.50 where prepared by conventional ceramic methods. Films were grown by pulsed laser deposition (PLD) in a high vacuum chamber by focusing a pulsed *KrF* excimer laser beam operating at 10 Hz onto a dithering and rotating target, as described elsewhere. [7] The film compositions and thicknesses were determined by Rutherford Backscattering Spectroscopy (*RBS*). X-ray diffraction patterns were collected using a rotating anode source and a conventional $\theta - 2\theta$

geometry. The Hall effect was measured on PLD films patterned into five-contact geometry, using a high temperature insert into a 20 Tesla superconducting magnet in the National High Magnetic Field Laboratory at Los Alamos, NM. The magnetization (M) and resistivity (ρ) were determined using standard SQUID techniques and the four probe method in an LHe dewar equipped with an 8 Tesla superconducting magnet, respectively.

Fig.1(a) displays the normalized resistance *vs* temperature for ceramic samples. The resistance peaks near the ferromagnetic transition temperature (see inset) and its temperature dependence, an exponential function with activation energy $E_\sigma \sim 140\ meV$, is only weakly dependent on the rare-earth content. The ferromagnetic phase transition temperature T_c is $\sim 255\ K$ in the pure sample, drops to $\sim 95\ K$ for $x = 0.25$, and it is not present for $x = 0.50$. This decrease agrees very well with experimental values found in Y-substituted samples. [6] The saturation magnetization in high fields for sample $x = 0$ agrees, within the error in the mass determination (5%), with the expected value for a doping level of 0.33 holes per unit cell. The sample corresponding to $x = 0.25$ shows an extra contribution to M at low temperatures which seems to follow a law $\chi_{DC} = C/(T + \theta)$ characteristic of antiferromagnetic ordering, with a Néel temperature $T_N < 2K$ probably related to the Gd magnetic moments. Fig.1(b) displays the thermopower (S) *vs* temperature for the same group of samples. The sensitivity of the thermopower to the metal-to-semiconductor phase transition is remarkable, showing characteristics of an authentic phase transition. In the high temperature regime, S is well described with the expression

$$S = \frac{k_B}{e}\left(\frac{E_s}{k_B T}\right) + S_\infty \qquad (1)$$

with S_∞ being a negative constant and E_s a characteristic energy in the range of $4 - 20$ $meV \ll E_\sigma$. Fits using Eq.(1) are displayed superimposed over data in Figs.1(b) and 2(b). The low temperature regime is characterized by an almost temperature independent, metal-like thermopower $|S_M| \sim 2\ \mu V/K$. Neither the sign of S_M nor the value of S_∞ are well understood assuming nominal compositions in the samples. Both oxygen and cationic (La, Mn) vacancies certainly play an important role and new studies are under way in order to

clarify this point. [8]

Fig.2(a) shows the resistivity for, 0.5 μm thick, film samples corresponding to compositions $x = 0.0$, 0.25 and 0.50. The most prominent difference between ceramics and films is a higher transition temperature in sample $x = 0.25$. X-ray data indicate that the in-plane Gd-induced lattice contraction of the laser ablated films is less pronounced than in the ceramic, presumably due to stress caused by the $LaAlO_3$ substrate. Such an effect places this sample closer to the pure system. This figure also display a fit with the adiabatic expession $\rho \propto T \exp(E_\sigma / k_B T)$ for sample $x = 0.25$, as an example, obaining $E_\sigma = 145\ meV$. Fig.2(b) shows the thermopower *vs* temperature for the same group of film samples. Ceramic results are reproduced. We estimated the magnitude of the drift mobility prefactor from the resistivity; its relatively high value ($\mu_d^o \equiv \sigma_o / ne \simeq 6\ cm^2/V\ s$ at room temperature in sample $x = 0.25$) indicates that the carrier motion is adiabatic. [4]

In order to find further experimental data to confirm the small-polaron picture we performed Hall effect experiments on PLD films. The temperature dependence of the Hall mobility of small polarons was calculated to be exponential, with an activation energy equal to one third that of the drift mobility. [4,9] The original calculation, assuming a positive transfer integral J for electrons hopping on a triangular lattice, also predicts a negative sign Hall coefficient (R_H). When holes are considered, however, both the carrier and J change signs leaving $R_H < 0$ (electron-like) and therefore anomalous. Although the application of this simple triangular model to the cubic Mn lattice may sound inappropriate, in fact the observed deviation from 180° Mn-O-Mn bonds guarantees a finite probability for face diagonal hopping.

The experimental results for film samples corresponding to $x = 0.0$ and 0.25 are displayed in Fig.3. The Hall coefficient was found to be negative and is plotted as $-R_H$ *vs* T. Data on sample $x = 0$ has relatively large error bars (not shown for clarity) due to its high magnetoresistance in the experimental temperature range. Sample $x = 0.25$ was measured, and smaller error bars were obtained, at temperatures between $2T_c$ and $4T_c$. $|R_H|$ decreases monotonically with temperature and was plotted in two different insets: (a) as $1/R_H$ *vs*

T and (b) as $\ln|R_H|$ *vs* $1000/T$. Even within the given experimental error it is clear in inset (a) that R_H does *not* have the temperature dependence of the susceptibility (expected to follow a Curie-Weiss law, with $T_c = 140$ K), ruling out in this way the presence of an extraordinary Hall effect. In inset (b) we observe an Arrhenius-like behavior, following a law $R_H = R_H^o \exp(E_H/k_B T)$ where R_H^o is a negative constant in the studied temperature range. The observed values for the activation energies for the conductivity in the adiabatic regime [10] $E_\sigma^A = 145\ meV$ and the Hall coeficient $E_H = 91 \pm 5\ meV$ give $E_H/E_\sigma^A = 0.64 \pm 0.03$ for sample $x = 0.25$, in excellent agreement with the theoretical prediction for small polarons $E_H/E_\sigma = 2/3$. However, the experimental prefactor ($R_H^0 = -3.8 \times 10^{-11}\ m^3/C$) leads to a hole density $n \simeq 3 \times 10^{22}\ cm^{-3}$ within the triangular lattice model , significantly larger than the nominal doping level of $5 \times 10^{21}\ cm^{-3}$.

In conclusion, we have measured the thermopower, resistivity and the high-temperature Hall coefficient in polycristalline ceramic and PLD film samples of composition $(La_{1-x}Gd_x)_{2/3}Ca_{1/3}MnO_3$ and found that the behavior of these magnitudes in the paramagnetic state can be understood if the charge carriers are small polarons that move by adiabatic hopping in the Mn sublattice. The essential physics is contained in the triangular lattice small polaron model by Holstein, Emin and Friedman. The sign anomaly in the Hall effect within this interpretation implies that small polarons hop among near-neighbor sites with a significant probability of traversing Hall-effect loops with odd numbers of legs. As such, the results indicate the occurrence of significant transfer across face diagonals, and therefore a crucial role for deviations of the *Mn-O-Mn* bond angle from 180°. The appropriate extension of this model to a realistic geometry in order to account for the expected carrier concentration is under consideration and will be discussed elsewhere. [10]

We would like to acknowledge the assistance of P. White on experimental aspects of this work and Dr. A. Lacerda at NHMFL, LANL. This research was supported in part by DOE Grant No. DEFG02-91ER45439 through the Illinois Materials Research Laboratory, by NSF Grant No. DMR 91-20000 through the Science and Technology Center for Superconductivity and by Los Alamos National Laboratory through a Berndt Matthias Fellowship (MBS).

REFERENCES

[1] K. Chahara, T. Ohno, M. Kasai and Y. Kozono, *Appl. Phys. Lett.* **63**, 1990 (1993). S. Jin, T. H. Tiefel, M. McCormack, R.A. Fastnacht, R. Ramesh and L.H. Chen, *Science*, **264**, 413 (1994).

[2] D. Emin, M. Hillery and N-L.H. Liu, Phys. Rev. B **33**, 2933 (1986).

[3] M. Jaime, M.B. Salamon, K. Pettit, M. Rubinstein, R.E. Treece, J.S. Horwitz, D.B. Chrisey *Appl. Phys. Lett.* **68**, 1576 (1996). M. Jaime et al., *Phys. Rev. B* (in press).

[4] L. Friedman and T. Holstein, *Ann. Phys.* **21**, 494 (1963). D. Emin and T. Holstein, *Ann. Phys.* **53**, 439 (1969).

[5] Y. Tokura, A. Urushibara, Y. Moritomo, T. Arima, A. Asamitsu, G. Kido and N. Furukawa, *J. Phys. Soc. Jap.* **63**, 3931 (1994).

[6] H.Y. Hwang, S-W. Sheong, P.G. Radaelli, M. Marezio, and B. Batlogg, *Phys. Rev. Lett.* **75**, 914 (1995).

[7] R.E. Treece, P. Dorsey, M. Rubinstein, J.M. Byers, J.S. Horwitz, E. Donovan and D.B. Chrisey, *Mat. Res. Soc. Symp. Proc.* **384**, 427 (1995).

[8] M. Jaime, P. Lin, M.B. Salamon, F. Prado and A. Caneiro, unpublished.

[9] D. Emin, *Phil. Mag.* **35**, 1189 (1977).

[10] M. Jaime, H. Hardner, M.B. Salamon, M. Rubinstein, P. Dorsey and D. Emin, unpublished.

FIG. 1 (a) The resistance *vs* temperature normalized to its value at $T = 320\ K$ for ceramic samples of composition $x = 0$ (thick line), $x = 0.25$ (■ : H = 0; dotted: H = 4 Tesla; □ : H = 8 Tesla) and $x = 0.5$ (thin line). The behavior is exponential, with activation energies close to 140 meV. Inset: The nominally zero field magnetization *vs* T. (b) The thermopower *vs* temperature. The dashed lines are fits with Eq.(1) in the high temperature range, giving values $S_\infty = -23, -54$ and $-56\ \mu V/K$ and $E_s = 4, 15, 18\ meV$ for samples $x = 0, 0.25$ and 0.5 respectively.

FIG. 2 (a) The electrical resistivity *vs* T for *PLD* films $x = 0, 0.25$ and 0.5 in zero field, showing the transition phase temperatures somewhat higher than in ceramics. $\rho(T)$ was fitted with the adiabatic expression described in the text and its activation energy, $E_\sigma = 145$ meV for $x = 0.25$, is weakly dependent on x. (a) The thermopower *vs* temperature showing 1/T behavior above T_c. The dashed lines are fits with Eq.(1) in the high temperature range, giving values $S_\infty = -42$ and $-50\ \mu V/K$ and $E_s = 8$, and 14 meV for samples with compositions $x = 0.25$ and 0.5 respectively.

FIG. 3. The Hall coefficient *vs.* T for film samples $x = 0$ (□) and $x = 0.25$. Data at each temperature were taken by sweeping the magnetic field from -16 T to 16 T (▲), and then from 16 T to -16 T (▼) over a period of several hours. The dashed line correspond to a fit of the form $R_H = R_H^0 \exp[E_H/k_B T]$ obtaining an activation energy $E_H = (91 \pm 5)\ meV$. Insets (a): $1/R_H$ vs. T showing an extrapolation to $245\ K \gg T_c = 142\ K$. (b) $\ln|R_H|$ *vs.* $1000/T$ showing the linearity of the data.

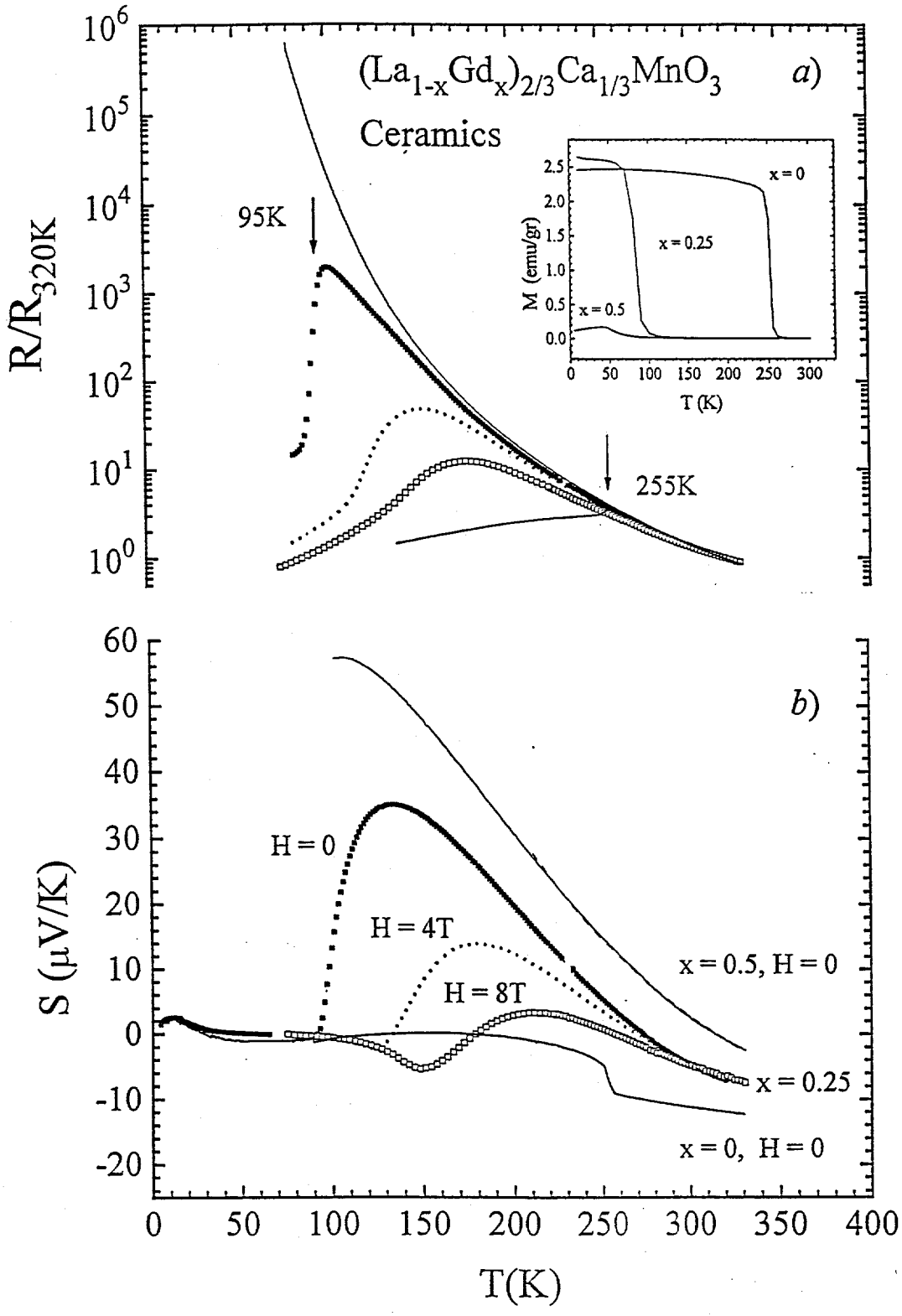
$(La_{1-x}Gd_x)_{2/3}Ca_{1/3}MnO_3$
a)
Ceramics
95K
255K
R/R_{320K}
M (emu/gr)
x = 0
x = 0.25
x = 0.5
T (K)
b)
H = 0
H = 4T
H = 8T
x = 0.5, H = 0
x = 0.25
x = 0, H = 0
S (μV/K)
T(K)

Figure 1

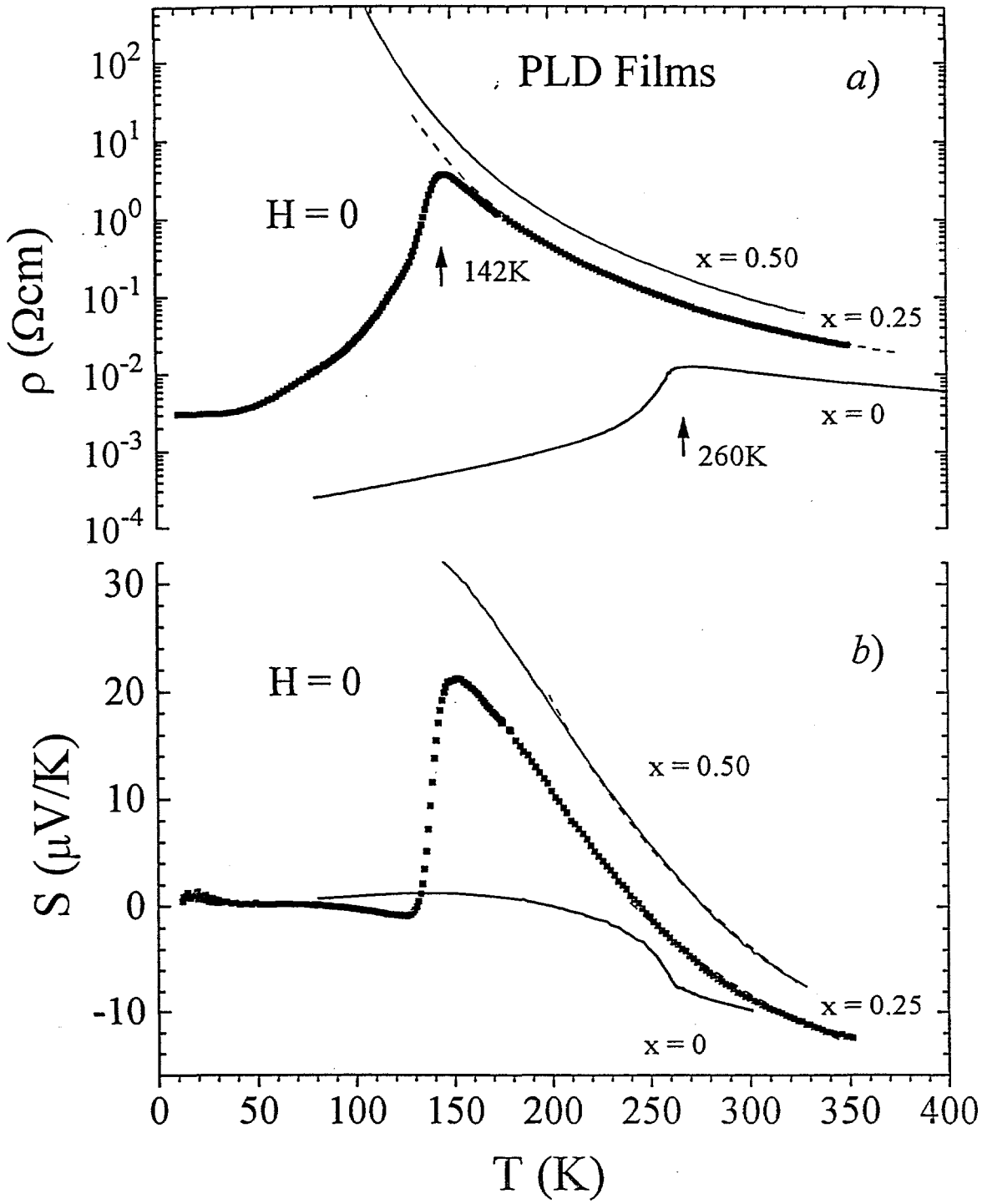
PLD Films
a)
H = 0
142K
x = 0.50
x = 0.25
x = 0
260K
ρ (Ωcm)
10^2
10^1
10^0
10^{-1}
10^{-2}
10^{-3}
10^{-4}
b)
H = 0
x = 0.50
x = 0.25
x = 0
S (μV/K)
30
20
10
0
-10
0
50
100
150
200
250
300
350
400
T (K)

Figure 2

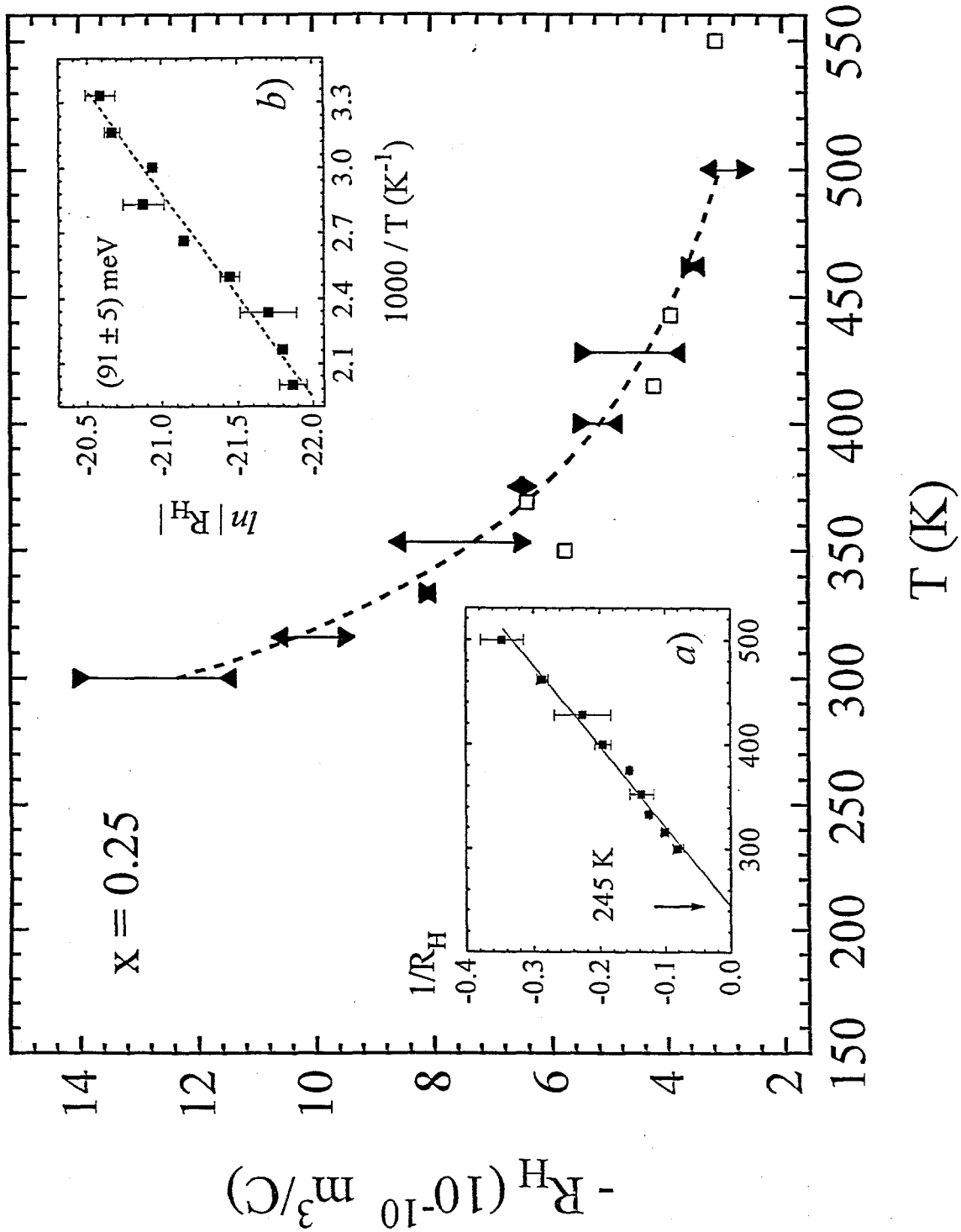

Figure 3